Interdigitated Sensing and Electrochemical Impedance Spectroscopy

Chapter 3

Interdigitated Sensing and Electrochemical Impedance Spectroscopy

Abstract This chapter elucidates the working principle of the different sensor prototypes that have been explained in the subsequent chapters. The electrodes of all the sensors were shaped in an interdigitated manner, working on the capacitive principle. Due to the flexible and interdigital nature of the sensors, the developed prototypes displayed dual nature of functionality. They were operated as electrochemical sensors with different solutions and as strain strains as a result of a change in dimensions with induced pressure. The sensors were conjugated with electrochemical impedance spectroscopy to determine the changes in impedance values with respect to different inputs provided as per specific applications.

3.1 Introduction

The working principle in accordance with the structure of the sensors is explained in this chapter. It describes the changes in their electrical and mechanical behavior with respect to different inputs. The sensor prototypes were fabricated to serve a dual purpose in terms of the mechanical changes with respect to the applied force, as well as the electrical changes when they were used in an electrochemical cell. It also explains the phenomenon of impedance spectroscopy that was used to characterize the sensor patches and subsequently determine the changes take place during different operations. The sensor prototypes were flexible in nature contained with interdigitated electrodes. The electrical conductivity of the sensors was dependent on the processed material used to develop electrodes, while their mechanical diversion was decided by the fabrication process used to form them. The electrodes of all the sensor prototypes were developed to be the same due to the distinct advantages mentioned in the

followed section of this chapter. Electrochemical impedance spectroscopy (EIS) was used as the computational tool in accordance with the fabricated prototypes to determine the changes for each application. The response of each of the systems was analyzed as a function of frequency to determine the changes occurring in linear and non-linear systems. EIS served as an excellent tool for measurement, as the sensors functioned at dynamic interfaces where specific system parameters were examined.

3.2 Planar Interdigital Sensors

Flexible sensor prototypes with an interdigital pattern were chosen for designing the electrodes. The electrodes were formed in an interdigitated manner due to certain advantages like their non-destructive and non-invasive manner of operation, generating rapid responses to the input changes (Ngo et al. 2016), high sensitivity of the sensor is as a result of the high change in the net electric field due to the different dielectric solutions and applied stress (Matsuzaki and Todoroki 2007) and minimized self-resonant frequency of the sensors as a result of the planar shape of the electrodes.

The sensor patches operated on capacitive sensing, where one electrode which is provided the voltage is named as excitation electrode, and the other one is termed as a reference electrode. The planar structure of the developed electrodes formed prototypes for single-sided and non-invasive measurements. Figure 3.1 shows the working principle of the designed electrodes (Khan and Kang 2015). When a frequency-depended voltage signal is applied to the excitation electrode, a resultant electric field is generated between the two oppositely charged electrodes. The electric field bulges from one electrode to another due to the planar nature of the electrodes. In order to determine The presence of the input material above the sensing area was determined via opting a one-directional measurement condition through the insulation of the other side of the substrate. When a material is considered for experimental purposes, it is positioned in contact with or in propinquity to the sensing area of the sensors. The field while bulging from one electrode to another of opposite polarity, penetrates through this Material Under Test (MUT). The properties of the electric field are changed as a result of penetration, which is

subsequently studied using any of the response analyzers to determine the dynamics of the system (Mukhopadhyay and Gooneratne 2007). In accordance with the changes in the stimulus to the system or device, the corresponding changes in the characteristics of the electric field are analyzed to determine the changes in the MUT. The penetration depth of the electric field is altered by altering the spatial wavelength (distance between the electrodes of the same polarity), which makes it a favorable option for domestic (Nag et al. 2016), industrial (Zia et al. 2011; Zia et al. 2014; Zia et al. 2015) and scientific (Afsarimanesh et al. 2017; Afsarimanesh et al. 2016; Alahi et al. 2018) applications.

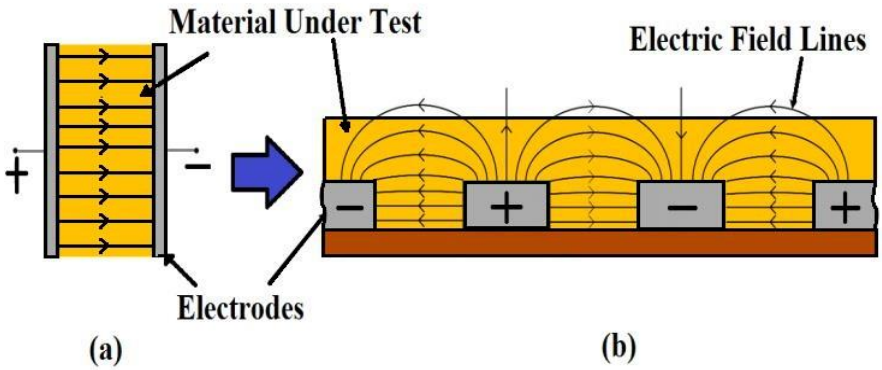

Figure 0.1 Working principle of the sensor patch. (a) The sensor works on the idea of a parallel-plate capacitor. (b) Due to the planar structure of the electrodes, the electric field bulges from one electrode to another of opposite polarity (Khan and Kang 2015).

Due to the flexibility of the sensor prototypes, there is a subsequent change in their responses as a result of the applied stress. The working principle for the developed sensor prototypes is shown in Figure 3.2. The interdigitated sensor replicates a parallel-plate capacitive device where the capacitance of the sensor depends on certain parameters shown in equation 3.1,

$$C \; \alpha \; {}^{(\in_o * \in_r * A)}/_{d} \qquad (3.1)$$

where C represents the capacitance, $\in_o$ = 8.85 × 10^{-12} F·m^{-1} represents the permittivity of vacuum, $\in_r$ represents the relative permittivity, A represents the effective area (A >> d), and d represents the effective spacing between electrodes of different polarity.

The change of d or A causes a change of the effective capacitance of the sensor. This can be utilized to analyze a physiological event through the change in resultant capacitance based on the cyclic deformation and reformation of the sensor patch. The exertion of a strain on the patch via a physiological event changes the value of the capacitance (Cai et al. 2013; Matsuzaki and Todoroki 2007). Figure 3.2 depicts the notion of the working principle of the sensors in terms of their response as a result of mechanical changes. L and W represent for the length and width of the sensor patches, respectively. ΔL, ΔW, and Δd are the effective changes in the length, width and interdigital distance of the sensor patch respectively when any deformation is caused on them.

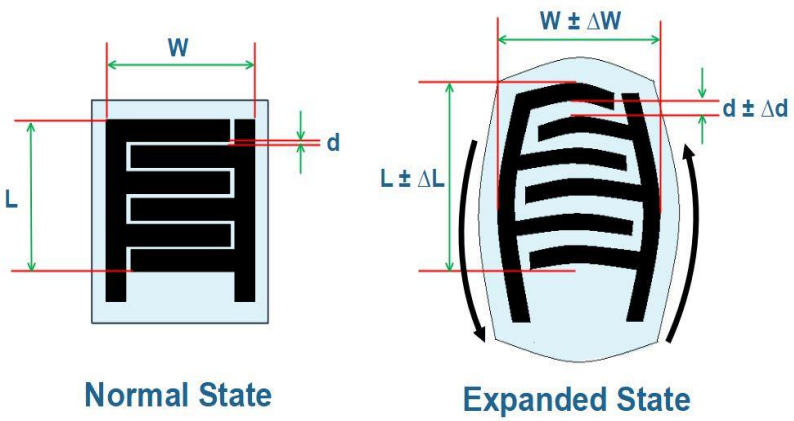

Figure 0.2 Operating principle of the developed sensor patches was based on the capacitive principle (Nag et al. 2018).

Using equation 3.1, the change in capacitance can be determined as a function of the changes in length (ΔL), width (ΔW) and interdigital distance (Δd) as depicted in equation 3.2,

$$\Delta C = C * (\frac{\Delta L}{L} + \frac{\Delta W}{W} - \frac{\Delta d}{d}) \quad (3.2)$$

where ΔC represents the change in capacitance; ΔL, ΔW and Δd are the changes in length, width and interdigital distance of the sensor patches respectively.

The effective reactive and impedance changes as a function of the changes in the resultant capacitance of the sensor patches:

$$\Delta X = f(\Delta C) \quad (3.3)$$

The strain exerted on the sensor patches leads to the reorientation of the nanofillers in the polymer matrix. This subsequently changes the resistance and as a result, the conductivity of the electrodes,

$$\Delta R = R * (\frac{\Delta l}{l} - \frac{\Delta A}{A} - \frac{\Delta \sigma}{\sigma}) \quad (3.4)$$

So, the overall changes in the impedance can be expressed as

$$\Delta Z = f(\Delta R, \Delta X) \quad (3.5)$$

where l represents the effective length of the electrodes, σ represents the effective conductivity, $\Delta\sigma$ represents the change in conductivity, ΔR, ΔX and ΔZ are the changes in the effective resistance, reactance and impedance respectively.

The change in the responses of the sensors can also be correlated to the change in the complex conductivity. The advantages of measuring the output in terms of conductivity are due to a couple of reasons. Firstly, for the high electrical conductivity of the electrodes, even a small change in dimension of the sensor prototype because of the applied strain can be analyzed in terms of conductivity. Secondly, the employment of the sensor prototypes for a range of applications that would exert different ranges of strain on them, as a result of which, the change in the conductivity of the electrodes can be studied

easily. Since the sensor prototypes are not ideal capacitors, the change in the conductivity values with respect to the change in frequency can be determined from the complex conductivity as shown from equation 3.6.

$$\sigma_{complex} = \sigma + j2\pi f\varepsilon \tag{3.6}$$

where $\sigma_{complex}$ is the complex conductivity, σ is the effective conductivity, ε is the permittivity, f is the operating frequency.

The electric-field density distribution for an applied strain between two consecutive electrode fingers of opposite polarity for one of the fabricated sensor prototypes is shown in Figure 3.3. The simulation was performed was done using COMSOL 3.2b. The simulation environment was taken to be vacuum while assigning graphite and PDMS as the electrode fingers and substrates of the sensor, respectively.

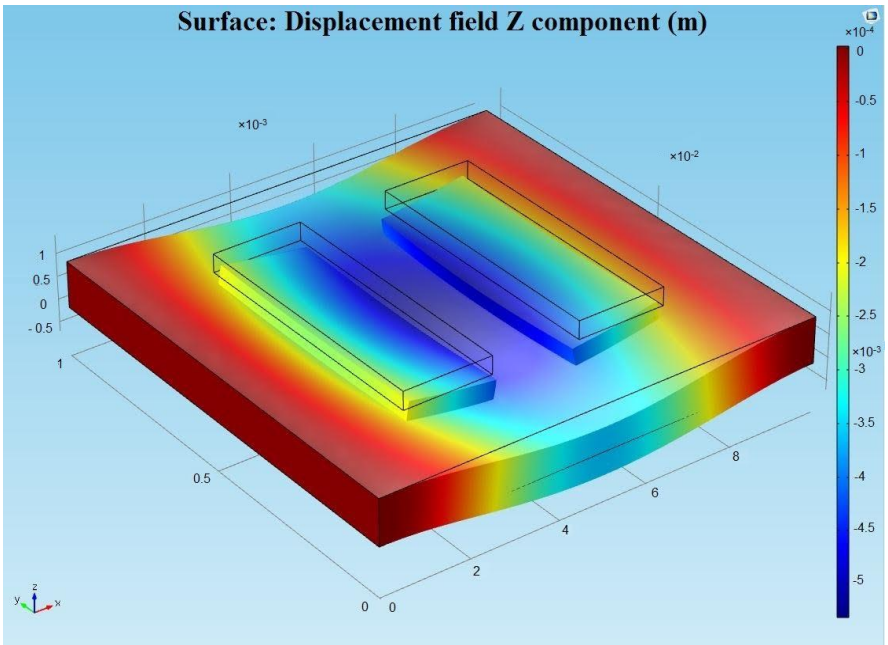

Figure 0.3 Three-dimensional simulation done using COMSOL 3.2b to determine the change in the electric field distribution on the sensor patch for the applied stress.

The electric field density was analyzed in terms of the displacement field in the same direction (z-direction) as that of the applied stress. The maximum electric field is being concentrated between the fingers, thus causing a maximum change around that region. Due to the capacitive nature of the sensor patches, the charge density on the electrode fingers varies with the resultant electric displacement field. So, the net charge density on the electrode fingers varies with the applied strain, thus causing a variation in their responses.

3.3 Electrochemical Impedance Spectroscopy (EIS)

Electrochemical Impedance Spectroscopy (EIS) is one of the most powerful mechanisms used for sensor investigations as a result of its robust and non-invasive nature (Lasia 2002). Although it is mostly used for characterizing the electrical double layer at the

electrode-electrolyte interfaces (Pajkossy and Jurczakowski 2017), the response of the sensors with respect to the change in frequency is also very useful in non-linear processes. EIS is a prominent technique with high resultant sensitivity towards the interfacial phenomenon that is used to analyze the changes in impedance of a cell in the presence of an external source. As a result, the frequency response analysis is performed in the presence of small amplitude of an AC signal on top of a controlled DC polarisation potential. The inner dynamics of the system are calculated from its responses towards the changes with respect to frequency. The resistive and reactive parts of the impedance values are generally considered to represent the changes happening inside a system. When an excitation voltage of small-amplitude is applied to a system, there is a corresponding change in the phase angle (Φ) between the input voltage and the output current of the system. This response is assumed to be pseudo-linear considering its change with respect to a low potential. In contrary, the linear system will generate a sinusoidal output current with respect to the input sinusoidal voltage with a shifted phase angle (Φ) as shown in Figure 3.4.

The excitation signal to an electrochemical cell can be represented as:

$$E_t = E_0 \sin \omega t \tag{3.7}$$

where E_t represents the output voltage at time t, E_0 represents the amplitude of the input signal, ω represents the angular frequency ($\omega = 2\pi f$) expressed in terms of radians/second, f represents the frequency in Hertz.

The output current of a linear circuit with a phase shift of Φ can be expressed as,

$$I_t = I_0 \sin(\omega t + \Phi) \tag{3.8}$$

Therefore, the total impedance can be expressed as,

$$Z = \frac{E_t}{I_t} = \frac{E_0 \sin \omega t}{I_0 \sin(\omega t + \theta)} \tag{3.9}$$

$$Z = Z_0 \frac{\sin(\omega t)}{\sin(\omega t + \theta)} \tag{3.10}$$

The responses from the sensor prototypes developed and deployed for different applications were monitored using different impedance analyzers. Physiological movements, tactile sensing, salinity, and nitrate sensing, force and strain measurements and taste senses are some of the applications the developed prototypes were employed. The response analyzers were tuned in accordance with a specific application, operating over a fixed or a specific frequency range. The connection of the analyzers to the system has been elucidated in the experimental section for each application.

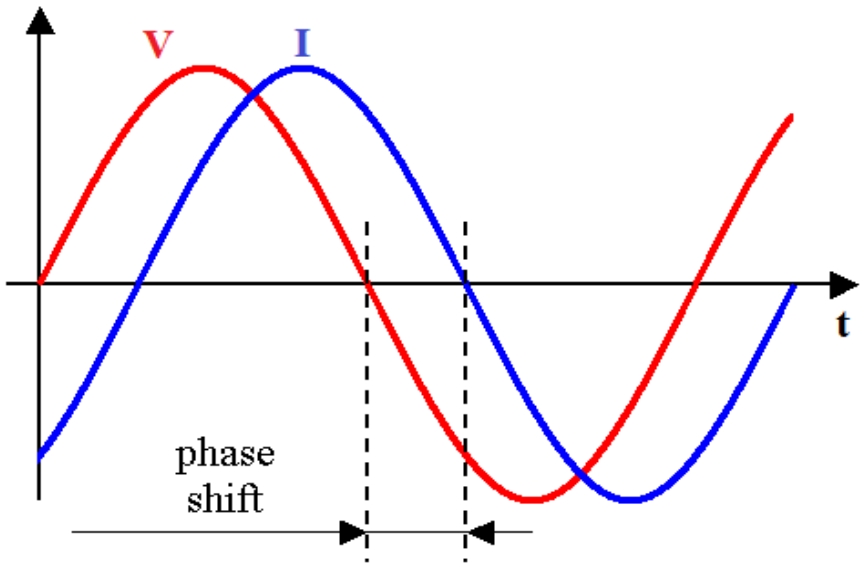

Figure 0.4 Phase shift in the output current with respect to the input voltage.

3.4 Conclusions

This chapter showcases the working principle of all the fabricated sensor prototypes. The flexible sensor patches were developed having

interdigitated electrodes which aided as in dual purposes in terms of their electrical and mechanical behavior. The electrical changes in the sensors occurred due to the interdigitated nature of the electrodes, while the mechanical modifications occurred as a result of their flexible nature. EIS was conjugated with the sensor prototypes to monitor their responses for each of the application. The response analyzers were chosen to perform the measurements for the linear and non-linear systems in the succeeding chapters.

3.5 References

Afsarimanesh N, Mukhopadhyay SC, Kruger M (2017) Molecularly Imprinted Polymer-Based Electrochemical Biosensor for Bone Loss Detection IEEE Transactions on Biomedical Engineering

Afsarimanesh N, Mukhopadhyay SC, Kruger M, Yu P-L, Kosel J Sensors and Instrumentation towards early detection of osteoporosis. In: Instrumentation and Measurement Technology Conference Proceedings (I2MTC), 2016 IEEE International, 2016. IEEE, pp 1-6

Alahi MEE, Nag A, Mukhopadhyay SC, Burkitt L (2018) A temperature-compensated graphene sensor for nitrate monitoring in real-time application Sensors and Actuators A: Physical 269:79-90

Cai L et al. (2013) Super-stretchable, transparent carbon nanotube-based capacitive strain sensors for human motion detection Scientific reports 3

Khan MRR, Kang S-W (2015) Highly sensitive multi-channel IDC sensor array for low concentration taste detection Sensors 15:13201-13221

Lasia A (2002) Electrochemical impedance spectroscopy and its applications. In: Modern aspects of electrochemistry. Springer, pp 143-248

Matsuzaki R, Todoroki A (2007) Wireless flexible capacitive sensor based on ultra-flexible epoxy resin for strain measurement of automobile tires Sensors and Actuators A: Physical 140:32-42

Mukhopadhyay SC, Gooneratne CP (2007) A novel planar-type biosensor for noninvasive meat inspection Sensors Journal, IEEE 7:1340-1346

Nag A, Afasrimanesh N, Feng S, Mukhopadhyay SC (2018) Strain induced graphite/PDMS sensors for biomedical applications Sensors and Actuators A 271:257-269

Nag A, Zia AI, Li X, Mukhopadhyay SC, Kosel J (2016) Novel Sensing Approach for LPG Leakage Detection—Part II: Effects of Particle Size, Composition, and Coating Layer Thickness IEEE Sensors Journal 16:1088-1094

Ngo T-T, Bourjilat A, Claudel J, Kourtiche D, Nadi M (2016) Design and Realization of a Planar Interdigital Microsensor for Biological Medium Characterization. In: Next Generation Sensors and Systems. Springer, pp 23-54

Pajkossy T, Jurczakowski R (2017) Electrochemical impedance spectroscopy in interfacial studies Current Opinion in Electrochemistry 1:53-58

Zia AI, Mohd Syaifudin A, Mukhopadhyay S, Al-Bahadly I, Yu P, Gooneratne C, Kosel J Development of Electrochemical Impedance Spectroscopy based sensing system for DEHP detection. In: Sensing Technology (ICST), 2011 Fifth International Conference on, 2011. IEEE, pp 666-674

Zia AI, Mukhopadhyay S, Al-Bahadly I, Yu P, Gooneratne CP, Kosel J Introducing molecular selectivity in rapid impedimetric sensing of phthalates. In: Instrumentation and Measurement Technology Conference (I2MTC) Proceedings, 2014 IEEE International, 2014. IEEE, pp 838-843

Zia AI, Mukhopadhyay SC, Yu P-L, Al-Bahadly IH, Gooneratne CP, Kosel J (2015) Rapid and molecular selective electrochemical sensing of phthalates in aqueous solution Biosensors and Bioelectronics 67:342-349